Strigolactones promote the localisation of the ABA exporter ABCG25 at the plasma membrane in root epidermal cells of Arabidopsis thaliana

Strigolactones promote the localisation of the ABA exporter ABCG25 at the plasma membrane in root epidermal cells of *Arabidopsis thaliana*

Giulia Russo[1, a], Serena Capitanio[1, 2, a], Marta Trasoletti[1], Cristina Morabito[1], Paolo Korwin Krukowski[1, 3], Ivan Visentin[1], Andrea Genre[2], Andrea Schubert[1], Francesca Cardinale[1]*

[1] PlantStressLab, DISAFA – University of Turin, Largo Braccini 2, I-10095 Grugliasco (TO), Italy

[2] DBIOS – University of Turin, Viale Mattioli 25, I-10125 Torino (TO), Italy

[3] Dipartimento di Bioscienze – University of Milan, via Celoria 26, I-20133 Milano, Italy

[a] These authors contributed equally to this work.

* Corresponding author, francesca.cardinale@unito.it

Giulia Russo [ORCID: 0000-0003-4762-3777] russogiulia84@gmail.com

Serena Capitanio [ORCID: 0000-0002-1609-0499] serena.capitanio@edu.unito.it

Marta Trasoletti [ORCID: 0000-0001-8125-8174] marta.trasoletti@unito.it

Cristina Morabito [ORCID: 0000-0003-4239-0492] cristina.morabito@unito.it

Paolo Korwin Krukowski [ORCID: 0000-0002-8973-2368] paolo.korwin@unimi.it

Ivan Visentin [ORCID: 0000-0002-5803-9034] ivan.visentin@unito.it

Andrea Genre [ORCID: 0000-0001-5029-6194] andrea.genre@unito.it

Andrea Schubert [ORCID: 0000-0001-7355-5865] andrea.schubert@unito.it

Francesca Cardinale [ORCID: 0000-0001-9892-9325] francesca.cardinale@unito.it

HIGHLIGHT

For the first time, strigolactones and ABA are proven to crosstalk in roots at the level of ABA transport across the cell membrane, in response to osmotic conditions.

ABSTRACT

The phytohormones strigolactones crosstalk with abscisic acid (ABA) in acclimation to osmotic stress, as ascertained in leaves. However, our knowledge about underground tissues is limited, and null in Arabidopsis. Namely, if strigolactones affect ABA transport across plasma membranes has never been addressed. We evaluated the effect of strigolactones on the localisation of ATP BINDING CASSETTE G25 (ABCG25), an ABA exporter in *Arabidopsis thaliana*. Wild-type, strigolactone-insensitive and -depleted seedlings expressing a GFP:ABCG25 construct were treated with ABA or strigolactones, and GFP was quantified by confocal microscopy in different subcellular compartments of epidermal root cells. We show that strigolactones promote the localisation of an ABA transporter at the plasma membrane by enhancing its endosomal recycling. Genotypes altered in strigolactone synthesis or perception are not impaired in ABCG25 recycling promotion by ABA, which acts downstream or independent of strigolactones in this respect. Additionally, we confirm that osmotic stress decreases strigolactone synthesis in *A. thaliana* root cells; and that such decrease may support local ABA retention under low water availability, by allowing ABCG25 internalisation. Thus, a new mechanism for ABA homeostasis regulation is proposed in the context of osmotic stress acclimation: the fine tuning by strigolactones of ABCG25 localisation in root cells.

KEYWORDS

Abscisic acid, ABCG25, *Arabidopsis thaliana*, GR24^{5DS}, endocytosis, osmotic stress, roots, strigolactones

ABBREVIATIONS

ABA: abscisic acid

ABCG25: ATP BINDING CASSETTE G 25

AIT1: IMPORTING TRANSPORTER 1

BFA: Brefeldin A

D14: DWARF 14

DTX50: DETOXIFICATION EFFLUX CARRIER 50

GFP: GREEN FLUORESCENT PROTEIN

MAX: MORE AXILLARY GROWTH

MS: Murashige and Skoog

NCED3: NINE-CIS-EPOXYCAROTENOID DIOXYGENASE 3

RD29B: RESPONSIVE TO DESICCATION 29B

RT: room temperature

TUA4: TUBULIN 4

UBQ10: UBIQUITIN 10

INTRODUCTION

Strigolactones have emerged in the past years as a class of plant hormones with a role in root and shoot development (Kelly *et al.*, 2023), plant interaction with (micro)organisms (Lanfranco *et al.*, 2018), and stress responses, among which acclimation to osmotic stress (Cardinale *et al.*, 2018; Trasoletti *et al.*, 2022). Strigolactones are synthesised by several enzymes acting sequentially on the all-*trans*-β carotene precursor. The core module of this pathway includes the isomerase DWARF (D) 27, and the carotenoid cleavage oxygenases MORE AXILLARY GROWTH (MAX) 3 and MAX4; these produce the key intermediate carlactone. Further modification of carlactone by other enzymes — mainly, but not only, members of the CytP450 family — eventually lead to canonical and non-canonical strigolactones, the blend of which is often species-specific. Strigolactone perception involves their binding to the α/β-fold hydrolase D14, which triggers a signalling cascade eventually de-repressing strigolactone responses (Cardinale *et al.*, 2018; Trasoletti *et al.*, 2022).

Water stress induces the transcription of strigolactone biosynthetic genes in the leaves of all tested dicots (Ha *et al.*, 2014; Liu *et al.*, 2015; Lv *et al.*, 2018; Visentin *et al.*, 2016), suggesting a positive role for endogenous strigolactones in alleviating drought stress at the shoot level. In fact, several lines defective in strigolactone signalling or biosynthesis have a reduced survival rate to drought, along with increased stomatal conductance, transpiration, and water loss (Ha *et al.*, 2014; Korwin Krukowski *et al.*, 2022; Li *et al.*, 2020; Liu *et al.*, 2015; Lv *et al.*, 2018; Marzec *et al.*, 2020; Visentin *et al.*, 2020; Visentin *et al.*, 2016; Zhang *et al.*, 2018). Consistently, exogenous strigolactones applied in the absence of stress are also capable of directly and transiently promoting stomatal closure (Lv *et al.*, 2018; Min *et al.*, 2019; Visentin *et al.*, 2020). By only apparent contrast, exogenous strigolactone treatment prior to or during stress was shown to maintain stomata open, with the consequence of sustaining photosynthesis, by boosting antioxidant metabolism and thus alleviating metabolic damage (Trasoletti *et al.*, 2022). In agreement with the general picture, strigolactone treatments increase plant survival rates to water stress (Ha *et al.*, 2014; Min *et al.*, 2019; Sedaghat *et al.*, 2021; Sedaghat *et al.*, 2017).

An obvious mechanistic possibility for the effects of strigolactones on stomatal regulation is interaction with abscisic acid (ABA) metabolism or signal. The strigolactone-ABA relationship is organ-dependent (Cardinale *et al.*, 2018). In general, plants with strigolactone-related defects display a shoot ABA content equal to or lower than wild-type plants under normal and/or stress conditions, along with a general reduction in ABA sensitivity that is thought to contribute heavily to stomatal opening and higher water loss (Bu *et al.*, 2014; Ha *et al.*, 2014; Li *et al.*, 2020; Liu *et al.*, 2015; Marzec *et al.*, 2020; Visentin *et al.*, 2020; Visentin *et al.*, 2016). However, a strong ABA-independent signature is also detectable in strigolactone effects under stress, both at the

transcriptome level and in the above-mentioned short-term promotion of stomatal closure in *Arabidopsis thaliana* (Arabidopsis) by exogenous strigolactones (Ha *et al.*, 2014; Li *et al.*, 2020; Lv *et al.*, 2018).

A different picture emerges in the root system, where drought stress represses the biosynthesis of strigolactones, which in turn negatively impacts ABA levels. This link between strigolactones and ABA biosynthesis was convincingly demonstrated in *Lotus japonicus*: pre-treatment with a synthetic strigolactone analogue blocks the transcriptional activation of the ABA biosynthetic gene *NINE-CIS-EPOXYCAROTENOID DIOXYGENASE 2* (*NCED2*) in the root, and local ABA accumulation in response to osmotic stress (Liu *et al.*, 2015). Thus, in non-mycorrhizal roots of dicots experiencing osmotic stress, a drop in strigolactone levels and exudation may be a prerequisite for local ABA rise (Liu *et al.*, 2015; Ruiz-Lozano *et al.*, 2016; Visentin *et al.*, 2016). It is however unknown whether this local effect is conserved in other plants, namely in Arabidopsis. Furthermore, no information is available on the possible effects of strigolactones on ABA transport across the cell membrane, and whether this affects ABA levels in roots.

ABA membrane transport in Arabidopsis root tissues involves the ABA exporter ATP-BINDING CASSETTE G25 (ABCG25). Under osmotic stress, ABCG25 translocates from the plasma membrane to the endosome compartment by enhanced endocytosis (Park *et al.*, 2016). In turn, this is proposed to reduce ABA export, tuning endocellular ABA concentration to the level required for the induction of downstream responses to stress. These include metabolic shifts to produce antioxidants and osmoprotectants, and for the promotion of root plasticity (Harris, 2015; Rowe *et al.*, 2016; Sharma *et al.*, 2019). In line with this hypothesis, exogenous ABA application was shown to increase the recycling of endosome-associated ABCG25 and its accumulation at the plasma membrane, likely to discharge excess ABA in the apoplast and regain hormonal homeostasis (Park et al., 2016).

In this study, we investigated whether strigolactone levels affect ABCG25 localisation in Arabidopsis root cells, under normal and osmotic stress conditions. To this aim, we expressed a soluble GREEN FLUORESCENT PROTEIN (GFP) fusion to ABCG25 in genetic backgrounds defective in strigolactone synthesis or perception, to compare protein localisation under stress and no-stress conditions. Also, the effects of treatment with a synthetic strigolactone analogue were tested in the same experimental system. Our results support the hypothesis that the build-up of endocellular ABA levels in response to osmotic stress in roots requires a decrease in basal strigolactone levels. This is strongly suggested also by our observation of decreased activity in the strigolactone biosynthetic pathway in roots under osmotic stress, and by the quantification of total ABA content in roots of wild-type plants and plants defective in ABCG25 availability, when treated with exogenous strigolactones and/or suffering osmotic stress.

MATERIALS AND METHODS

Plant material and growth conditions

Arabidopsis thaliana (L.) Heynh. plants were grown in a culture room under short-day conditions: 8 hours (h) photoperiod, 22°C day, 18°C night, 40-50% relative humidity, and light intensity *c.* 150 µmol $m^{-2}s^{-1}$. Surface-sterilised seeds were vertically grown on half-strength Murashige and Skoog (0.5X MS) agarised medium (2.2 g/L MS basal salts, 1% sucrose, 0.8% agar) and used for confocal imaging and transcript quantification experiments 6 days after germination. The transgenic line expressing the translational fusion between ABCG25 and GFP under the control of the cassava vein mosaic virus (CsVMV) promoter in the wild-type Col-0 background (GFP:ABCG25/wt) had been previously described (Park *et al.*, 2016) and was kindly provided to our laboratory by Prof. Inhwan Hwanga from the Pohang University of Science and Technology, Korea. The *A. thaliana* T-DNA insertion lines used in this study were the *max3-11* (SALK_023975) (Auldridge *et al.*, 2006) and the *abcg25-5* (SALK_128873) (Merilo *et al.*, 2015) obtained from the NASC, and the *d14-1* (NASC ID: N913109) (Li *et al.*, 2020; Seto *et al.*, 2019; Waters *et al.*, 2012), which was kindly provided by Prof. Lam-Son Phan Tran from the RIKEN Center for Sustainable Resource, Japan (now at Texas A&M). All were genotyped with the primers listed in the **Supplementary Table S1**.

Generation of transgenic plants

GFP:ABCG25/*max3* and GFP:ABCG25/*d14* transgenic plants were obtained by crossing the GFP:ABCG25/wt plants with the *max3-11* or *d14-1* lines. F1 plants were selected on agar plates supplemented with hygromycin (25 mg/L); F2 plants were screened at the stereomicroscope for GFP fluorescence in the root apex and subjected to PCR genotyping (**Supplementary Table S1**). Homozygous F3 plants were then used for treatments and *in vivo* imaging.

Hormonal, chemical, and osmotic stress treatments

For hormonal treatments, vertically grown seedlings were immersed for 4 h in liquid 0.5X MS medium containing acetone 0.1% (v/v) for control (mock) conditions, 10 µM ABA (Sigma-Aldrich) or 10 µM $GR24^{5DS}$ (StrigoLab Srl; active stereoisomer of the strigolactone biosynthetic analogue GR24) (Scaffidi *et al.*, 2014). For Brefeldin A (BFA; Sigma-Aldrich) treatments, seedlings were treated at a final concentration of 50 µM using a 100 mM stock prepared in DMSO. For BFA washouts, seedlings pre-treated with BFA for 1 h were transferred to new 0.5X MS medium modified with acetone, ABA or $GR24^{5DS}$ as above for different time lengths, as reported in figure legends. To check whether strigolactones could influence the expression of the *GFP:ABCG25* transgene or of endogenous *AtABCG25*, GFP:ABCG25/wt and wild-type plants were vertically grown in 0.5X MS agar plates and 16-day-old seedlings were sprayed with 10 µM $GR24^{5DS}$ or 0.1% acetone water solution. Roots were

sampled after 4 h and frozen in liquid nitrogen for further analyses. Four biological replicates were generated for each condition, each obtained by pooling together the roots of 20 seedlings.

To apply osmotic stress for confocal observations, seedlings grown on vertical 0.5X MS plates were carefully peeled off and immersed in sterile distilled water or 20% (w/v) polyethylene glycol (PEG 8000; Sigma-Aldrich) for different time lengths, as reported in figure legends. To quantify total ABA in roots, the wild type and *abcg25-5* mutant were vertically grown in agar plates as described above. After 4 weeks, plantlets were sprayed with 10 µM $GR24^{5DS}$ solution, while controls were sprayed with a 0.1% solution of acetone in water; 24 h later, osmotic stress was induced by spraying a 20% PEG solution while controls were sprayed with water. Roots were sampled 24 h later and frozen in liquid nitrogen. Four biological replicates were generated for each condition, each replicate being the pool of root apparatuses from 20 seedlings.

Confocal microscopy and image analyses

A Leica TCS SP2 confocal microscope (Milan, Italy) equipped with a long-distance 40X water-immersion objective (HCX Apo 0.80; Leica Microsystems GmbH, Wetzlar, Germany) was used for the imaging of epidermal and cortical cells in the root division zone. Both GFP and the red fluorescent lipophilic dye FM4-64 were excited using an argon laser band of 488 nm and fluorescence emission was recorded between the 510–540 nm for GFP and 600-700 nm for FM4-64. To track endocytosis, the GFP:ABCG25 transgenic seedlings were incubated on ice for 5 minutes (min) in a 0.5X MS staining solution containing 4 µM of FM4-64, and root epidermal cells were imaged 5 min or 3 h after endocytosis was restarted by shifting to room temperature (RT). For the visualization of BFA bodies, seedlings were first pre-treated with 50 µM BFA for 30 min at RT and then stained with FM4-64 for 5 min on ice (Rigal *et al.*, 2015).

All images of control and treated seedlings were acquired with the same microscope settings. Images were analysed using the FIJI/ImageJ software (Schindelin *et al.*, 2012) to calculate mean fluorescence intensity in the cytoplasm and plasma membrane for each cell. The ratio between these values was then used to compare the relative intensity of the two fluorescence signals between experimental conditions. At least 20 cells from 3 to 4 different biological replicates (individual seedlings) were quantified for each experimental condition, as specified in figure legends. Each hormonal, chemical or stress treatment for confocal observations was reproducibly and independently repeated at least three times.

ABA quantification

Twenty mg aliquots of lyophilized root samples were extracted in 1 ml of methanol/water (1:1) solvent for 20 min at 4°C, using an ultrasonic bath. After centrifugation, the obtained supernatant was transferred to a 2 ml glass vial for ABA quantification on a C-18 HPLC column and a LC-MS 8045 (Shimadzu, Japan). ABA concentrations were determined using a calibration standard curve (1-0,5-0,2-0,1-0,05-0,01-0,005-0,001 ppm) of pure ABA. Deuterated ABA was added to each sample and standard as an internal analytical control.

Gene transcript quantification

At least three biological replicates of *A. thaliana* root tissues were generated for each condition, pooling together rootlets from over 50 6-day-old seedlings (*c.* 40 mg). Samples were snap-frozen in liquid nitrogen and mechanically disrupted in a TissueLyser system (Qiagen Retsch GmbH, Hannover, Germany). Total RNA was isolated using the RNeasyTM Mini kit (Qiagen, Hilden, Germany); RNA quality and quantity were assessed photometrically. After DNase I treatment (New England Biolabs; NEB), DNA contamination was ruled out by conventional PCR on the α-Tubulin-encoding gene *AtTUA4* (**Supplementary Table S1**), and single-strand cDNA synthesised with the M-MLV RT enzyme (ThermoFisher). Specific primers for quantitative RT (qRT)-PCR analyses of *GFP* (for transgene expression), *AtMAX3*, *AtMAX4*, *AtRD29B*, *AtNCED3* and *AtABCG25* were retrieved from literature or designed using the Primer3 tool (https://primer3.org) (**Supplementary Table S1**). qRT-PCR experiments were carried out in the StepOne system (Applied Biosystems, ThermoFisher) using the following programme: 1 min preincubation at 95°C, followed by 40 cycles of 15 s at 95°C, and 30 s at 60°C. All reactions were performed with three analytical replicates, and only when standard deviation did not exceed 0.3 were Ct values considered. The comparative threshold cycle method (Rasmussen, 2001) was used to calculate relative expression levels based on the geometric means of values from *AtTUA4* and the ubiquitin-encoding gene *AtUBQ10* (**Supplementary Table S1**).

Accession Numbers

Gene sequences in this article can be found in the Arabidopsis Information Resource or the GenBank/EMBL databases, and other data libraries under the accession numbers or IDs listed in **Supplementary Table S1**.

Data analyses

Statistical tests were carried out after running a preliminary parametric test of normal data distribution: Student's t-tests for comparison of averages between two samples, or one-way analysis of variance for multiple comparisons (One-Way ANOVA) or yet Three-way when interactions among

variables were to be assessed, with a probability level threshold for significance of $P < 0.05$. Otherwise, the Wilcoxon rank sum test or the Kruskall-Wallis test was used. All statistical analyses were performed with the R statistical package (http://www.r-project.org).

RESULTS

Exogenous strigolactones induce the accumulation of ABCG25 at the plasma membrane

To test the hypothesis that strigolactones may modulate ABA membrane transport, we first examined whether high levels of exogenous strigolactones affect the subcellular localisation of the ABA transporter ABCG25 in root tips of *A. thaliana*. To achieve this, we took advantage of seedlings carrying a GFP fusion with ABCG25 (GFP:ABCG25/wt line). The correct localisation of the fusion protein at the plasma membrane and in endosomes (Park *et al.*, 2016) was first confirmed by staining our samples with the lipophilic dye FM4-64 for 5 min (**Supplementary Fig. S1**) and 3 h (not shown) after the restart of endocytosis by shifting from ice to RT. For hormonal treatments, transgenic seedlings were immersed in liquid media containing different hormonal solutions, and the ratio of average GFP intensity in the cytosol over the plasma membrane was quantified by confocal microscopy followed by image analysis. Our observations highlighted a marked increase in GFP emission at the plasma membrane when roots were exposed for 4 h to the strigolactone synthetic analogue $GR24^{5DS}$, in comparison to mock treatments (**Fig. 1**). Quantitative image analysis confirmed a statistically significant decrease in the cytosol/plasma membrane ratio; importantly, this decrease was stronger in the root tips treated with $GR24^{5DS}$ than ABA, which is known to induce ABCG25 accumulation at the plasma membrane and was used as a positive control (**Fig. 1**) (Park *et al.*, 2016). Of note, $GR24^{5DS}$ treatment did not change GFP-ABCG25 transcripts significantly in the GFP:ABCG25/wt line (quantified with GFP-targeted primers), nor in the wild type (**Supplementary Fig. S2**). This indicates that strigolactones do not affect constitutive transgene expression nor the expression of endogenous *ABCG25* in our setup; however, they promote ABCG25 accumulation at the plasma membrane, at least as efficiently as ABA.

Endogenous strigolactones promote cell membrane localisation of ABCG25

To assess whether endogenous strigolactones could influence the subcellular localisation of ABCG25, we inserted the GFP:ABCG25 construct into *max3-11* plants by crossing them to GFP:ABCG25/wt, to generate the GFP:ABCG25/*max3* line. *MAX3* (At2g44990) encodes a key enzyme in the synthesis of the strigolactone precursor carlactone, and *max3-11* shows a 70–75% reduction in strigolactone content (Alder *et al.*, 2012; Booker *et al.*, 2004). We observed that in the absence of any treatment, GFP:ABCG25/*max3* plants displayed more abundant GFP-labelled endosomes compared to the wild

type, reflected in an increase of the cytosol/plasma membrane fluorescence ratio in the strigolactone-depleted line compared to the wild type (**Fig. 2A**). We incubated the GFP:ABCG25/*max3* seedlings in mock or hormone-containing solutions and quantified the subcellular localisation of the GFP fluorescence after 4 h. In analogy to our observations in the wild-type, ABA treatment of *max3-11* seedlings caused a significant decrease in the cytosol/plasma membrane fluorescence ratio compared to mock-treated controls (**Fig. 2B**), showing that exogenous ABA-dependent accumulation of ABCG25 at the membrane was not changed in the presence of low endogenous strigolactone levels in *max3-11* seedlings. A comparable increase in plasma membrane fluorescence was observed upon $GR24^{5DS}$ treatment of GFP:ABCG25/*max3* seedlings (**Fig. 2B**), indicating that a 10 µM supply of exogenous strigolactone analogue is sufficient to compensate for the low endogenous strigolactone levels of this line. We then expressed the GFP:ABCG25 construct in the *d14-1* genotype (GFP:ABCG25/*d14* line). *D14* (At3g03990) codes for the α/β hydrolase that perceives endogenous strigolactones, and *d14-1* displays a strigolactone-insensitive phenotype in both seedlings and adult plants (Waters, Nelson et al. 2012, Seto, Yasui et al. 2019, Li, Nguyen et al. 2020). First, we investigated if the impairment in strigolactone perception could affect the subcellular localisation of ABCG25, comparing GFP fluorescent signals between GFP:ABCG25/wt and GFP:ABCG25/*d14* lines in the absence of any treatment. As observed with *max3-11*, the results confirmed decreased GFP signal at the plasma membrane in the *d14-1* background (**Fig. 2C**). When challenged with ABA, the GFP:ABCG25/*d14* line relocated ABCG25 to the plasma membrane to a comparable level to the wild-type and *max3-11* background, while it did not do so in the presence of $GR24^{5DS}$ (**Fig. 2C**).

Altogether, these results confirm that the effects of $GR24^{5DS}$ on ABCG25 localisation depend on the strigolactone receptor, and that endogenous strigolactones have the same effect as $GR24^{5DS}$. They also suggest that ABA impacts on ABCG25 localisation downstream or independently of strigolactones.

Exogenous strigolactones enhance ABCG25 recycling from the endosomes

The ABA-dependent accumulation of ABCG25 at the plasma membrane has been linked to enhanced recycling from endosomes rather than endocytosis inhibition (Park *et al.*, 2016). On this basis, we decided to investigate whether the same occurred in our seedlings upon $GR24^{5DS}$ treatment. To this aim, we first measured the endocytosis rate in sGFP:ABCG25/wt seedlings after a 4 h pre-treatment with hormones or mock solutions, followed by 30 min in a BFA solution. BFA is a fungal toxin that blocks exocytosis; under BFA treatment, endocyted proteins accumulate in so-called BFA bodies in the cytoplasm. For this reason, BFA has been extensively used to dissect endocytic processes (Renna and Brandizzi, 2020). We observed that the GFP signal localises to BFA bodies under all hormonal

conditions, with no significant differences in cytosol/plasma membrane signal ratios (**Fig. 3A**). On this basis, we concluded that exogenous strigolactones, like ABA, do not influence the ABCG25 endocytosis rate. When rootlets were stained with FM4-64 after incubation in the BFA solution, a partial co-localisation of the two signals was observed at BFA bodies, confirming the endosomal nature of these vesicles (**Supplementary Fig**. **S3A**).

We then checked whether the GR24^{5DS}-induced accumulation of ABCG25 at the plasma membrane was related to enhanced protein recycling from endosomes. To this aim, we measured the rate of GFP disappearance from the BFA bodies at different time points during toxin washout with hormone-containing or mock solutions after BFA treatments. As shown in **Fig. 3B**, 1 h after transfer to mock or hormone-containing media, GFP fluorescence in BFA bodies decreased in all cases, while it significantly increased at the plasma membrane of hormone-treated seedlings compared to controls, with no significant difference between ABA and GR24^{5DS} treatments. Eventually, 2 h after washout initiation, a maximum increase in GFP signal was recorded at the plasma membrane alongside an almost complete disappearance in BFA bodies-associated fluorescence. This effect was particularly marked in the GR24^{5DS}-treated seedlings (**Fig. 3B**).

Taken together, these observations suggest that exogenous strigolactones may modulate ABA homeostasis in root epidermal cells by enhancing ABCG25 recycling from the endosomes to the plasma membrane, similarly to the reported effects of ABA itself (Park *et al.*, 2016).

Endogenous strigolactones promote ABCG25 recycling from endosomes to the plasma membrane

To highlight the cellular mechanisms that allow the GR24^{5DS}-induced increase of ABCG25 at the plasma membrane in the wild type but are blocked in the strigolactone-insensitive line, we repeated the BFA washout experiments on the *d14-1* line. When rootlets were incubated for 30 min in the BFA solution and stained with FM4-64, a consistent co-localization of the two signals was observed at BFA bodies, as in the wild type (**Supplementary Fig**. **S3B**). Notably, the cytosol/plasma membrane fluorescence ratio after BFA incubation showed that ABCG25 accumulated at BFA bodies more intensely in the *d14-1* genotype than in the wild-type (**Supplementary Fig. S3C**), suggesting that the constitutive endocytosis of ABCG25 is rather promoted by the lack of strigolactone perception in the *d14-1* genotype.

In the washout experiment, *d14-1* seedlings exhibited a decrease of the cytosol/plasma membrane ratio of GFP fluorescence after a 4 h-long treatment with ABA (**Fig. 4**), as observed in the wild-type background (**Fig. 3B**). By contrast, when BFA was washed out with a mock or GR24^{5DS} solution, the decrease in fluorescence of BFA bodies was significantly slower, and BFA bodies remained clearly visible after 2 h in both conditions. Unlike the wild type, the cytosol/plasma membrane fluorescence

ratio in the *d14-1* background remained high after washout with $GR24^{5DS}$ when compared to ABA (**Fig. 4**). Thus, the lack of strigolactone perception in the *d14-1* genotype blocks, as expected, the $GR24^{5DS}$-induced accumulation of ABCG25 at the plasma membrane, but not the effects of ABA on the same process — a conclusion in line with our previous observations in the absence of BFA treatment (**Fig. 2**).

Collectively, these results confirm the dependency of $GR24^{5DS}$ effects from the strigolactone receptor and support the hypothesis that ABA acts on ABCG25 localisation downstream or independent of strigolactones. They also show that strigolactones do not affect the general endosome recycling mechanisms, as ABCG25 recycling in the presence of a high concentration of exogenous ABA is not affected in the *d14-1* line.

Osmotic stress down-regulates strigolactone biosynthetic genes in *A. thaliana* roots

During drought and osmotic stress (e.g., imposed by PEG), a decrease in strigolactone content, accompanied by the downregulation of the biosynthetic genes *CCD7* and *CCD8,* was observed in the roots of *Lotus japonicus, Solanum lycopersicum* and lettuce (Liu *et al.*, 2015; Ruiz-Lozano *et al.*, 2016; Visentin *et al.*, 2016). Currently, no data are available on the expression of these genes in Arabidopsis roots exposed to osmotic stress conditions.

To obtain this information, 6-day-old *A. thaliana* seedlings were immersed in a solution containing 20% PEG or in water for 30 min, 1 or 3 h before roots were sampled for RNA extraction. The transcript levels of the strigolactone biosynthetic genes *MAX3* and *MAX4* were quantified in these samples, revealing a significant reduction in comparison to mock-treated samples at the same time point, and to the pre-stress levels (**Fig. 5**). A strong induction of the ABA biosynthetic gene *9-CIS-EPOXYCAROTENOID DIOXYGENASE3* (*NCED3*) (Iuchi *et al.*, 2001) and of the ABA-responsive gene *RD29B* (*RESPONSIVE TO DEHYDRATION29B*) (Yamaguchi-Shinozaki and Shinozaki, 1993), both well known to respond to stress conditions (Liu *et al.*, 2015; Msanne *et al.*, 2011), was also observed. By contrast, *ABCG25* transcripts were observed to increase only later in our experimental setup, 3 h after stress start (**Fig. 5**).

These findings confirm that PEG-induced osmotic stress causes the early (within 30 min) transcriptional activation of ABA responses and the simultaneous repression of strigolactone biosynthetic genes in *A. thaliana* roots, in analogy with other dicots.

Osmotic stress promotes faster ABCG25 endocytosis in the strigolactone-insensitive line *d14-1* than in wild-type Arabidopsis

We then wondered whether the osmotic stress-induced drop in strigolactone synthesis could be functional to ABCG25 localisation dynamics, i.e., to the internalisation of ABCG25 in the lytic vacuole as proposed by Park *et al.* (2016) to prevent ABA export and promote its accumulation in root cells. Since *d14-1* roots show more abundant GFP:ABCG25-tagged endosomes than the wild type in the absence of any treatment (**Fig. 2A**), we considered the possibility that the constitutive lack of endogenous strigolactone perception promotes a faster ABCG25 internalisation than the drop in strigolactone synthesis during the onset of osmotic stress. We therefore treated *A. thaliana* seedlings with either 20% PEG or water (as mock treatment) and compared the cytosol/plasma membrane GFP fluorescence ratio in the wild-type and *d14-1* background 1, 2 and 3 h after the beginning of the experiment.

Firstly, our observations confirmed that the mean fluorescent signal ratios between cytosol and plasma membrane are higher in PEG-treated than in control wild-type roots for each time point, as previously described (Park *et al.*, 2016) (**Fig. 6A**). Secondly, we also observed this effect in the strigolactone-insensitive line *d14-1* (**Fig. 6B**). Thus, ABCG25 endocytosis rate grew over time in both genotypes under PEG conditions, as the cytosolic GFP signal started to increase together with the accumulation of intracellular fluorescent vesicular-like structures until it labelled the vacuolar compartments at later time points. This indicated that the PEG-induced internalisation of ABCG25 (which involves vesicular trafficking from the plasma membrane to the vacuole) is a progressive process that is not inhibited by the lack of strigolactone perception. Furthermore, we found that seedling immersion in water (mock treatment) also determined fluctuations of plasma membrane fluorescence in both genotypes (mock-treated samples in **Fig. 6A, B**). Thus, to compare the kinetics of ABCG25 endocytosis between the two genotypes in this setup, we normalised the cytosol/plasma membrane ratio of the GFP signal in each PEG-treated sample to the respective mock-treated control for every time point (**Fig. 6C**). After 1 h, the normalised ratio was significantly higher in the *d14-1* background compared to the wild type, while during the following 2 h the ratio in the wild type progressively increased until at 3 h, it reached the levels recorded in *d14-1*. As visible in the confocal images, this is most likely due to the higher number of GFP-labelled endosomes in the strigolactone-insensitive seedlings both before stress (**Fig. 2A**) and as soon as 1 h after the beginning of the stress treatment, while the wild type started accumulating labelled endosomes later. In fact, a clear and diffused vacuolar GFP labelling was visible in the *d14-1* background as soon as 2 h from the beginning of PEG treatment (**Fig. 6A, B**). Staining with FM4-64 confirmed that PEG treatment caused

the endocytosis of GFP:ABCG25, visible at endosomes at early stages and at vacuole at late stages (**Supplementary Fig. S4**).

Together, these results indicate that the lack of strigolactone perception in the *d14-1* background accelerates ABCG25 endocytosis during the early (< 2 h) response to osmotic stress. In turn, this suggests on the one hand that basal levels of strigolactones in the roots can initially inhibit PEG-induced ABCG25 internalisation triggered by stress, and on the other hand that the downregulation of the strigolactone biosynthetic pathway, observed in roots as an early response to osmotic stress, may promote ABCG25 internalisation.

Exogenous strigolactones modulate ABA levels in roots, partly in dependence of ABCG25

We finally checked whether keeping artificially high the levels of strigolactones in roots would change total ABA levels in Arabidopsis roots, both in the absence and presence of osmotic stress, and whether their effect, if any, would depend on ABCG25 presence. To this aim, 4-week-old *in vitro*-grown plantlets of the wild-type and *abcg25-5* mutant genotype were treated with $GR24^{5DS}$ or a mock solution, and 24 h later they were sprayed with 20% PEG. After 24 additional hours, total ABA was quantified. As shown in **Fig. 7**, osmotic stress did not induce any quantifiable change in total root ABA, in either genotype. This is in line with what already reported in Arabidopsis (Christmann *et al.*, 2005). Treatment with synthetic strigolactone, on the other hand, tended to increase total ABA levels in the wild type, especially if followed by 24 h of osmotic stress, even if not significantly. In the *abcg25-5* mutant background, instead, ABA levels were seen dropping after $GR24^{5DS}$ treatment compared to untreated controls (both stressed and unstressed), while PEG treatment partially recovered this drop. Also, of note, steady-state levels of total ABA were higher in the *abcg25-5* mutant than in the wild type, in the absence of hormonal treatments (**Fig. 7**). Indeed, the three-way ANOVA analysis here performed confirmed a significant interaction among the genotype and the $GR24^{5DS}$ treatment ($P = 0.04$).

DISCUSSION

Strigolactones modulate ABA homeostasis in root cells by promoting ABCG25 localisation at the plasma membrane via endosomal recycling

In this study, we determined that the levels of ABCG25 at the plasma membrane correlate with strigolactone content and signalling. Indeed, treatment with the synthetic analogue $GR24^{5DS}$ on wild-type Arabidopsis plants expressing the GFP:ABCG25 fusion shows lower cytosol/plasma membrane ratios of ABCG25 in root epidermal cells, than mock-treated samples. The same occurs when plants

are treated with the positive control ABA, as cells need to pump out the hormone to control its homeostasis (Park *et al.*, 2016). Consistently, we observed that ABCG25 was relatively less abundant in the plasma membrane of the strigolactone-depleted line *max3-11* and the strigolactone-insensitive *d14-1.* Also, *max3-11* re-localised ABCG25 at the plasma membrane when supplied with $GR24^{5DS}$ to compensate and exceed the lack of endogenous strigolactones. By contrast — and as expected — the lack of strigolactone perception in *d14-1* roots prevented the increase of ABCG25 at the plasma membrane following treatment with $GR24^{5DS}$. This effect of $GR24^{5DS}$ seems to be prominently non transcriptional in our setup, as neither endogenous ABCG25 nor transgene transcripts were changed by treatment. It may be interesting to also note in this regard that in grape (Vitis vinifera) berries, the basal transcript levels of the putative *ABCG25* orthologue are also not changed by *rac*-GR24. The latter however reduces *ABCG25* transcriptional activation by ABA (Ferrero *et al.*, 2018). Thus, even though *rac*-GR24 is less specific to D14-dependent signalling than $GR24^{5DS}$, we cannot exclude that in different experimental conditions, strigolactones may indeed also alter *ABCG25* expression.

The localisation and turnover of many transporter proteins is determined by the constitutive subcellular trafficking of vesicles between the plasma membrane and the endosomes. In fact, endocytic cargos can return to the plasma membrane via a variety of interacting partners (González Solís *et al.*, 2022). Some hormones were already known to modulate their own homeostasis by stabilising the plasma membrane presence of their transporters, such as ABA with ABCG25 and auxin with PIN (PIN-FORMED) 1 (reviewed in (Park *et al.*, 2017), even though the underlying mechanisms are different for ABCG25 (activation of recycling from early endosomes) and PIN1 (inhibition of endocytosis). Strigolactones, in this picture, were already known to interfere with the polar targeting, constitutive trafficking as well as clathrin-mediated endocytosis of the auxin transporters PIN (Kumar *et al.*, 2015; Zhang *et al.*, 2020). We demonstrate here that recycling of ABCG25 from endosomes to the plasma membrane appears also to be promoted by strigolactones, since ABCG25 moved from the BFA bodies to the plasma membrane faster if $GR24^{5DS}$ was present during BFA washout. Such an effect by $GR24^{5DS}$ is dependent on an intact strigolactone perception pathway, as it was abolished in the *d14-1* background. Instead, neither endogenous nor exogenous strigolactones promoted the ABCG25 endocytosis; if anything, lack of strigolactone perception slightly but significantly increased endocytosis. Again, this scenario is reminiscent of what was observed by Park *et al.* (2016) — and confirmed here — in the presence of excess ABA.

Our results collectively show that under irrigated conditions, ABA homeostasis in roots — which is also dependent on the localisation of its ABCG25 exporter — is influenced not only by ABA itself but

also by strigolactones; and suggest that the latter may negatively influence ABA intracellular levels in root tissues by increasing its export from root cells.

Changes in strigolactone levels in the roots may modulate local ABA homeostasis during osmotic stress

The role of strigolactones in Arabidopsis response to drought and osmotic stress had previously been elucidated by works mostly focused on leaves and stomatal cells, and on strigolactone effects on ABA levels and sensitivity in the leaves (Ha *et al.*, 2014; Lv *et al.*, 2018). Nonetheless, it has been shown in *Lotus japonicus* that osmotic stress represses strigolactone biosynthesis in the roots: a decrease in strigolactone contents in both root exudates and tissues is accompanied by a fast transcriptional repression of the genes encoding strigolactone biosynthetic enzymes. A similar drop has been reported in non-mycorrhizal roots of both lettuce and tomato plants under osmotic stress, also proving a clear correlation between the downregulation of strigolactone biosynthetic genes and metabolites (Liu *et al.*, 2015; Ruiz-Lozano *et al.*, 2016; Visentin *et al.*, 2016). Low strigolactones in roots are needed for the transcriptional de-repression of a key ABA biosynthetic gene and for ABA rise under osmotic stress, and thus, may be a pre-requisite for root acclimation to stress in this species (Liu *et al.*, 2015). In the present study, we report that in 6–day-old Arabidopsis roots the upregulation of the ABA biosynthetic gene *NCED3* and of the ABA-responsive gene *RD29B* is accompanied by the downregulation of the strigolactone biosynthetic genes *MAX3* and *MAX4*, as soon as 30 min after the beginning of a PEG-induced osmotic stress that progressively continues until 3 h. This confirms that the repression of strigolactone synthesis in plant roots is a common organ-specific response mechanism to osmotic stress, shared among dicots — Arabidopsis included.

It has been shown that both saline (NaCl) and osmotic (PEG) stresses cause the removal of ABCG25 from the plasma membrane of root epidermal cells, followed by endocytosis and transport to the vacuole. Based on these observations, ABCG25 internalisation has been proposed as a mechanism by which root cells likely increase endocellular ABA concentrations, in addition to the activation of ABA biosynthetic genes (Park *et al.*, 2016). In our hands, total ABA content in root tissues was not affected by PEG treatment; however, transcription of *RD29B*, a marker of ABA-dependent responses, is dramatically activated (**Fig. 7** and **5**). This is consistent with previous findings (Rowe *et al.*, 2023) and suggests that under stress, a relocation strategy that makes more ABA available for endocellular perception while not changing total levels may be at play; this may happen by means also of ABCG25 internalisation, as proposed earlier (Park *et al.*, 2016). Furthermore, as we showed that the ABCG25 localisation ratio of the strigolactone-insensitive genotype is shifted, under unstressed conditions, towards what happens during osmotic stress, we reasoned that the repression of strigolactone synthesis under stress might be important to achieve the right balance between ABA retention *vs*

extrusion in root tissues. Indeed, when the wild type was contrasted with *d14-1* plants, strigolactone-insensitive root cells displayed a decreased GFP signal at the plasma membrane due to a lower rate of ABCG25 recycling from the vacuole to the plasma membrane in the absence of any treatment; and a faster rate of ABCG25 internalisation at our earliest time point of PEG exposure (1 h). Thus, an accelerated re-localisation of ABCG25 to the root cell vacuole during osmotic stress could be observed in strigolactone-depleted or insensitive genotypes, with respect to the wild type. The difference between the two genotypes tended to decrease in the following two hours and disappeared at the end of the experiment, most likely due to strigolactone synthesis being meanwhile repressed in wild-type roots under stress. This supports the hypothesis that in Arabidopsis roots subjected to osmotic stress, a decrease in strigolactone synthesis in roots could favour the increase in endocellular ABA levels not only or not so much through the upregulation of ABA biosynthesis, as demonstrated in Lotus (Liu *et al.*, 2015) but rather through the re-localisation of its transporter (**Fig. 8**). This picture is also supported by the free ABA levels in wild-type and *abcg25-5* plants treated with $GR24^{5DS}$ and/or subjected to osmotic stress. In fact, $GR24^{5DS}$ tended to increase total ABA levels of otherwise unstressed wild-type roots; this suggests that the higher presence of ABCG25 at the plasma membrane makes less ABA available to perception, pushing the cells to produce more. Additionally, keeping the levels of strigolactones artificially high by a $GR24^{5DS}$ treatment prior to osmotic stress further increased total ABA root levels, as if the preferred strategy of ABCG25 internalisation for higher endocellular ABA were less effective, thus pushing the cells to produce more of the hormone to attain the needed endocellular levels. On the other hand, such $GR24^{5DS}$-triggered increase is not so obvious in the *abcg25-5* background, which will have no ABCG25 protein susceptible to strigolactone action (Fig. 7). This strongly suggests that the strigolactone-ABA crosstalk in Arabidopsis roots is indeed mediated by ABCG25 localisation dynamics, but quantifying endocellular ABA levels in stressed and unstressed roots upon treatment with $GR24^{5DS}$ will be necessary to directly address this question, for example by using the novel ABACUS2 biosensors (Rowe *et al.*, 2023).

Notably, NaCl induces ABCG25 internalisation also in the vascular tissue and endodermal region of the roots, while apparently not in companion cells, and this opens the possibility that in doing so it may affect root-to shoot ABA transport. However, no clear involvement of ABCG25 is reported in ABA loading to the phloem during abiotic stress (Park *et al.*, 2016), even if its gene is mainly expressed in the phloem companion cells in root tissues (Kuromori *et al.*, 2014). It must be recalled here that a rise in root ABA levels was initially hypothesised to feed its systemic export, and drought signalling to the aerial part (Comstock, 2002); in this light, a block in ABA extrusion from root cells to the vasculature during stress would be counter-productive for acclimation. However, the increase in

leaf ABA levels has been later found to be entirely due to local synthesis/release from storage, both in Arabidopsis and other herbaceous plants; during long-term stress, root ABA levels are even sustained by its synthesis in leaves rather than the opposite (Christmann *et al.*, 2007; Holbrook *et al.*, 2002; Manzi *et al.*, 2015). Thus, the higher stress-induced ABA availability to root cells is envisaged to not have systemic effects, but rather a local role in root stress acclimation: for example, in the promotion of osmoprotectant and antioxidant responses, as well as in root morphology remodelling (Harris, 2015; Rowe *et al.*, 2016; Sharma *et al.*, 2019).

Different implications for the organ-specific strigolactone-ABA interactions under stress

Besides being expressed in roots, aboveground the exporter ABCG25 is mainly expressed in phloem companion cells and is involved in ABA accumulation in guard cells (Kuromori *et al.*, 2016; Kuromori *et al.*, 2010; Kuromori *et al.*, 2014).

In the roots, the fact that ABA action on ABCG25 localisation is unaffected by decreased levels of endogenous strigolactones or their impaired perception tentatively places ABA downstream or independent of strigolactones in this process. Strigolactones are known to promote ABA sensitivity in the shoot (Cardinale *et al.*, 2018); even though this possibility has not been tested in root tissues yet, it may in principle be proposed as the mechanism by which strigolactones modulate ABCG25 localisation. Indeed, the recycling of ABCG25 from endosomes to the plasma membrane promoted by ABA is strongly impaired in an ABA-insensitive line (Park *et al.*, 2016), indicating that as expected, cytosolic ABA signalling plays a key role in this process. However, *de novo* ABA synthesis and perception are not needed for ABCG25 internalisation under high-salt stress (Park *et al.*, 2016), raising the interesting possibility that under stress, strigolactone effects on ABCG25 may be uncoupled from ABA signalling as well. Indeed, as mentioned in the introduction, strigolactones are known to act partly ABA-independently under stress (Cardinale *et al.*, 2018). Targeted experiments quantifying the recycling of ABCG25 in the ABA-insensitive genotype upon treatment with $GR24^{5DS}$ will be necessary to directly address this question.

In the shoot instead, the transcription of biosynthetic genes for strigolactones is repressed by root-produced strigolactones (Beveridge, 2006; Cardinale *et al.*, 2018; Trasoletti *et al.*, 2022). Thus, the reduced level of strigolactones in roots may be a component of the systemic drought signal, whereby local strigolactone synthesis in the leaves is de-repressed under osmotic stress (Visentin *et al.*, 2016). In this context, the fact that plants defective in strigolactone synthesis or perception display a clear drought-sensitive, rather than tolerant phenotype, is obviously justified by the shoot-specific increase of strigolactones during stress and their positive interaction with ABA levels and sensitivity (Cardinale *et al.*, 2018; Visentin *et al.*, 2016) and will override it in phenotypic assessments

of performances under stress. However, whether strigolactones affect cross-membrane ABA transport also in the leaf — where the hormone directly affects stomatal functioning and redox homeostasis — remains to be established; our experimental set-up is not amenable to observations in photosynthetic tissues (Park *et al.*, 2016).

Several ABA transporters besides ABCG25 may be modulated by strigolactones, both in roots and shoots. At the vasculature level, ABCG25 cooperates with the importer ABA-IMPORTING TRANSPORTER1 (AIT1) (Kanno *et al.*, 2012) to transport the hormone, while on the guard cell membrane, ABA import is mediated by ABCG40 (Kang *et al.*, 2010) and ABA export by DETOXIFICATION EFFLUX CARRIER50 (DTX50) (Zhang *et al.*, 2014). Each of them would be an interesting candidate for post-translational regulation by strigolactones, both at the shoot and root level.

ACKNOWLEDGEMENTS

The authors are thankful to Prof. Inhwan Hwang (Pohang University of Science and Technology, KR) for the kind gift of hemizygous GFP:ABCG25/wt plants, and Prof. Lam-Son Phan Tran (Texas A&M) for the *d14-1* genotype. They also wish to thank Dr. Lorenzo Borghi (University of Zurich, CH) for the purification of the homozygous GFP:ABCG25/wt line used in this work, and Dr. Daniela Minerdi for technical help.

AUTHOR CONTRIBUTIONS

GR and FC conceived of the work and designed the experiments helped by AG and AS. GR and SC performed the experiments and analysed the data, helped by MT, CM, PKK, IV. GR and FC drafted the manuscript, with contribution by all authors. IV, AG and AS critically reviewed the manuscript. All authors read, commented, and approved the final manuscript.

CONFLICT OF INTEREST

The authors declare no conflict of interest.

FUNDING

This work was supported by the European Union's Horizon 2020 research and innovation programme [grant agreements 727929 (TOMRES project) and 101000622 (RADIANT project)]; by the Horizon Europe Innovation Actions programme [grant agreement 101081858 (ECONUTRI project)]; and by PRIMA (VEG-ADAPT project), a programme supported by the European Union. None of these funding sources were involved in writing the manuscript. Open Access Funding provided by Università degli Studi di Torino within the CRUI-CARE Agreement.

DATA AVAILABILITY

The data supporting the findings of this study are available from the corresponding author, Francesca Cardinale, upon request.

REFERENCES

Alder A, Jamil M, Marzorati M, Bruno M, Vermathen M, Bigler P, Ghisla S, Bouwmeester H, Beyer P, Al-Babili S. 2012. The path from β-carotene to carlactone, a strigolactone-like plant hormone. Science **336**, 1348-1351.

Auldridge ME, Block A, Vogel JT, Dabney-Smith C, Mila I, Bouzayen M, Magallanes-Lundback M, DellaPenna D, McCarty DR, Klee HJ. 2006. Characterization of three members of the Arabidopsis carotenoid cleavage dioxygenase family demonstrates the divergent roles of this multifunctional enzyme family. The Plant Journal **45**, 982-993.

Beveridge CA. 2006. Axillary bud outgrowth: sending a message. Current Opinion in Plant Biology **9**, 35-40.

Booker J, Auldridge ME, Wills S, McCarty D, Klee H, Leyser O. 2004. MAX3/CCD7 is a carotenoid cleavage dioxygenase required for the synthesis of a novel plant signaling molecule. Current Biology **14**, 1232-1238.

Bu Q, Lv T, Shen H, Luong P, Wang J, Wang Z, Huang Z, Xiao L, Engineer C, Kim TH, Schroeder JI, Huq E. 2014. Regulation of drought tolerance by the F-box protein MAX2 in Arabidopsis. Plant Physiology **164**, 424-439.

Cardinale F, Korwin Krukowski P, Schubert A, Visentin I. 2018. Strigolactones: mediators of osmotic stress responses with a potential for agrochemical manipulation of crop resilience. Journal of Experimental Botany **69**, 2291-2303.

Christmann A, Hoffmann T, Teplova I, Grill E, Müller A. 2005. Generation of active pools of abscisic acid revealed by *in vivo* imaging of water-stressed Arabidopsis. Plant Physiology **137**, 209–219.

Christmann A, Weiler EW, Steudle E, Grill E. 2007. A hydraulic signal in root-to-shoot signalling of water shortage. Plant Journal **52**, 167-174.

Comstock JP. 2002. Hydraulic and chemical signalling in the control of stomatal conductance and transpiration. Journal of Experimental Botany **53**, 195-200.

Ferrero M, Pagliarani C, Novak O, Ferrandino A, Cardinale F, Visentin I, Schubert A. 2018. Exogenous strigolactone interacts with abscisic acid-mediated accumulation of anthocyanins in grapevine berries. Journal of Experimental Botany **69**, 2391-2401.

González Solís A, Berryman E, Otegui MS. 2022. Plant endosomes as protein sorting hubs. FEBS Letters **596**, 2288-2304.

Ha CV, Leyva-Gonzalez MA, Osakabe Y, Tran UT, Nishiyama R, Watanabe Y, Tanaka M, Seki M, Yamaguchi S, Dong NV, Yamaguchi-Shinozaki K, Shinozaki K, Herrera-Estrella L, Tran LS. 2014. Positive regulatory role of strigolactone in plant responses to drought and salt stress. Proceedings of the National Academy of Sciences, USA **111**, 851-856.

Harris JM. 2015. Abscisic acid: hidden architect of root system structure. Plants **4**, 548-572.

Holbrook NM, Shashidhar VR, James RA, Munns R. 2002. Stomatal control in tomato with ABA-deficient roots: response of grafted plants to soil drying. Journal of Experimental Botany **53**, 1503-1514.

Iuchi S, Kobayashi M, Taji T, Naramoto M, Seki M, Kato T, Tabata S, Kakubari Y, Yamaguchi-Shinozaki K, Shinozaki K. 2001. Regulation of drought tolerance by gene manipulation of 9-*cis*-Epoxycarotenoid Dioxygenase, a key enzyme in abscisic acid biosynthesis in Arabidopsis. The Plant Journal **27**, 325-333.

Kang J, Hwang J-U, Lee M, Kim Y-Y, Assmann SM, Martinoia E, Lee Y. 2010. PDR-type ABC transporter mediates cellular uptake of the phytohormone abscisic acid. Proceedings of the National Academy of Sciences, USA **107**, 2355-2360.

Kanno Y, Hanada A, Chiba Y, Ichikawa T, Nakazawa M, Matsui M, Koshiba T, Kamiya Y, Seo M. 2012. Identification of an abscisic acid transporter by functional screening using the receptor complex as a sensor. **109**, 9653-9658.

Kelly JH, Tucker MR, Brewer PB. 2023. The strigolactone pathway is a target for modifying crop shoot architecture and yield. Biology **12**, 95.

Korwin Krukowski P, Visentin I, Russo G, Minerdi D, Bendahmane A, Schubert A, Cardinale F. 2022. Transcriptome analysis points to BES1 as a transducer of strigolactone effects on drought memory in *Arabidopsis thaliana*. Plant & Cell Physiology **pcac058**.

Kumar M, Pandya-Kumar N, Dam A, Haor H, Mayzlish-Gati E, Belausov E, Wininger S, Abu-Abied M, McErlean CS, Bromhead LJ, Prandi C, Kapulnik Y, Koltai H. 2015. Arabidopsis response to low-phosphate conditions includes active changes in actin filaments and PIN2 polarization and is dependent on strigolactone signalling. Journal of Experimental Botany **66**, 1499-1510.

Kuromori T, Fujita M, Urano K, Tanabata T, Sugimoto E, Shinozaki K. 2016. Overexpression of AtABCG25 enhances the abscisic acid signal in guard cells and improves plant water use efficiency. Plant Science **251**, 75-81.

Kuromori T, Miyaji T, Yabuuchi H, Shimizu H, Sugimoto E, Kamiya A, Moriyama Y, Shinozaki K. 2010. ABC transporter AtABCG25 is involved in abscisic acid transport and responses. Proceedings of the National Academy of Sciences, USA **107**, 2361-2366.

Kuromori T, Sugimoto E, Shinozaki K. 2014. Inter-tissue signal transfer of abscisic acid from vascular cells to guard cells. Plant Physiology **164**, 1587-1592.

Lanfranco L, Fiorilli V, Venice F, Bonfante P. 2018. Strigolactones cross the kingdoms: plants, fungi, and bacteria in the arbuscular mycorrhizal symbiosis. Journal of Experimental Botany **69**, 2175–2188.

Li W, Nguyen KH, Chu HD, Watanabe Y, Osakabe Y, Sato M, Toyooka K, Seo M, Tian L, Tian C, Yamaguchi S, Tanaka M, Seki M, Tran LS. 2020. Comparative functional analyses of DWARF14 and KARRIKIN INSENSITIVE 2 in drought adaptation of *Arabidopsis thaliana*. The Plant Journal **103**, 111-127.

Liu J, He H, Vitali M, Visentin I, Charnikhova T, Haider I, Schubert A, Ruyter-Spira C, Bouwmeester HJ, Lovisolo C, Cardinale F. 2015. Osmotic stress represses strigolactone biosynthesis in *Lotus japonicus* roots: exploring the interaction between strigolactones and ABA under abiotic stress. Planta **241**, 1435-1451.

Lv S, Zhang Y, Li C, Liu Z, Yang N, Pan L, Wu J, Wang J, Yang J, Lv Y, Zhang Y, Jiang W, She X, Wang G. 2018. Strigolactone-triggered stomatal closure requires hydrogen peroxide synthesis and nitric oxide production in an abscisic acid-independent manner. New Phytologist **217**, 290–304.

Manzi M, Lado J, Rodrigo MJ, Zacarias L, Arbona V, Gomez-Cadenas A. 2015. Root ABA accumulation in long-term water-stressed plants is sustained by hormone transport from aerial organs. Plant and Cell Physiology **56**, 2457-2466.

Marzec M, Daszkowska-Golec A, Collin A, Melzer M, Eggert K, Szarejko I. 2020. Barley strigolactone signalling mutant *hvd14.d* reveals the role of strigolactones in abscisic acid-dependent response to drought. Plant, Cell & Environment **43**, 2239-2253.

Merilo E, Jalakas P, Kollist H, Brosché M. 2015. The role of ABA recycling and transporter proteins in rapid stomatal responses to reduced air humidity, elevated CO_2, and exogenous ABA. Molecular Plant **8**, 657-659.

Min Z, Li R, Chen L, Zhang Y, Li Z, Liu M, Ju Y, Fang Y. 2019. Alleviation of drought stress in grapevine by foliar-applied strigolactones. Plant Physiology and Biochemistry **135**, 99-110.

Msanne J, Lin J, Stone JM, Awada T. 2011. Characterization of abiotic stress-responsive *Arabidopsis thaliana RD29A* and *RD29B* genes and evaluation of transgenes. Planta **234**, 97-107.

Park J, Lee Y, Martinoia E, Geisler M. 2017. Plant hormone transporters: what we know and what we would like to know. BMC Biology **15**, 93.

Park Y, Xu Z-Y, Kim SY, Lee J, Choi B, Lee J, Kim H, Sim H-J, Hwanga I. 2016. Spatial regulation of ABCG25, an ABA exporter, is an important component of the mechanism controlling cellular ABA levels. The Plant Cell **28**, 2528–2544.

Rasmussen R. 2001. Quantification on the LightCycler. In: Meuer S, Wittwer C, Nakagawara K, eds. *Rapid Cycle Real-Time PCR*. Berlin, Heidelberg: Springer.

Renna L, Brandizzi F. 2020. The mysterious life of the plant *trans*-Golgi network: advances and tools to understand it better. Journal of Microscopy (Oxford) **278**, 154-163.

Rigal A, Doyle SM, Robert S. 2015. Live cell imaging of FM4-64, a tool for tracing the endocytic pathways in Arabidopsis root cells. Methods in Molecular Biology **1242**, 93-103.

Rowe JH, Topping JF, Liu J, Lindsey K. 2016. Abscisic acid regulates root growth under osmotic stress conditions via an interacting hormonal network with cytokinin, ethylene and auxin. New Phytologist **211**, 225-239.

Rowe J, Grangé-Guermente M, Exposito-Rodriguez M, Wimalasekera R, Lenz MO, Shetty KN, Cutler SR, Jones AM. 2023. Next-generation ABACUS biosensors reveal cellular ABA dynamics driving root growth at low aerial humidity. Nature Plants **9**, 1103–1115.

Ruiz-Lozano JM, Aroca R, Zamarreno AM, Molina S, Andreo-Jimenez B, Porcel R, Garcia-Mina JM, Ruyter-Spira C, Lopez-Raez JA. 2016. Arbuscular mycorrhizal symbiosis induces strigolactone biosynthesis under drought and improves drought tolerance in lettuce and tomato. Plant, Cell & Environment **39**, 441-452.

Scaffidi A, Waters MT, Sun YK, Skelton BW, Dixon KW, Ghisalberti EL, Flematti GR, Smith SM. 2014. Strigolactone hormones and their stereoisomers signal through two related receptor proteins to induce different physiological responses in Arabidopsis. Plant Physiology **165**, 1221-1232.

Schindelin J, Arganda-Carreras I, Frise E, Kaynig V, Longair M, Pietzsch T, Preibisch S, Rueden C, Saalfeld S, Schmid B, Tinevez J-Y, White DJ, Hartenstein V, Eliceiri K, Tomancak P, Cardona A. 2012. Fiji: an open-source platform for biological-image analysis. Nature Methods **9**, 676-682.

Sedaghat M, Emam Y, Mokhtassi-Bidgoli A, Hazrati S, Lovisolo C, Visentin I, Cardinale F, Tahmasebi-Sarvestani Z. 2021. The potential of the synthetic strigolactone analogue GR24 for the maintenance of photosynthesis and yield in winter wheat under drought: investigations on the mechanisms of action and delivery modes. Plants **10**, 1223.

Sedaghat M, Tahmasebi-Sarvestani Z, Emam Y, Mokhtassi-Bidgoli A. 2017. Physiological and antioxidant responses of winter wheat cultivars to strigolactone and salicylic acid in drought. Plant Physiology and Biochemistry **119**, 59-69.

Seto Y, Yasui R, Kameoka H, Tamiru M, Cao M, Terauchi R, Sakurada A, Hirano R, Kisugi T, Hanada A, Umehara M, Seo E, Akiyama K, Burke J, Takeda-Kamiya N, Li W, Hirano Y, Hakoshima T, Mashiguchi K, Noel JP, Kyozuka J, Yamaguchi S. 2019. Strigolactone perception and deactivation by a hydrolase receptor DWARF14. Nature Communications **10**, 191.

Sharma A, Shahzad B, Kumar V, Kohli SK, Sidhu GPS, Bali AS, Handa N, Kapoor D, Bhardwaj R, Zheng B. 2019. Phytohormones regulate accumulation of osmolytes under abiotic stress. Biomolecules **9**, 285.

Trasoletti M, Visentin I, Campo E, Schubert A, Cardinale F. 2022. Strigolactones as a hormonal hub for the acclimation and priming to environmental stress in plants. Plant, Cell & Environment **45**, 3611-3630.

Visentin I, Pagliarani C, Deva E, Caracci A, Turečková V, Novák O, Lovisolo C, Schubert A, Cardinale F. 2020. A novel strigolactone-miR156 module controls stomatal behaviour during drought recovery. Plant, Cell & Environment **43**, 1613-1624.

Visentin I, Vitali M, Ferrero M, Zhang Y, Ruyter-Spira C, Novak O, Strnad M, Lovisolo C, Schubert A, Cardinale F. 2016. Low levels of strigolactones in roots as a component of the systemic signal of drought stress in tomato. New Phytologist **212**, 954-963.

Waters MT, Nelson DC, Scaffidi A, Flematti GR, Sun YK, Dixon KW, Smith SM. 2012. Specialisation within the DWARF14 protein family confers distinct responses to karrikins and strigolactones in Arabidopsis. Development **139**, 1285-1295.

Yamaguchi-Shinozaki K, Shinozaki K. 1993. Arabidopsis DNA encoding two desiccation-responsive *RD29* genes Plant Physiology **101**, 1119–1120.

Zhang H, Zhu H, Pan Y, Yu Y, Luan S, Li L. 2014. A DTX/MATE-type transporter facilitates abscisic acid efflux and modulates ABA sensitivity and drought tolerance in Arabidopsis. Molecular Plant **7**, 1522-1532.

Zhang J, Mazur E, Balla J, Gallei M, Kalousek P, Medveďová Z, Li Y, Wang Y, Prát T, Vasileva M, Reinöhl V, Procházka S, Halouzka R, Tarkowski P, Luschnig C, Brewer PB, Friml J. 2020. Strigolactones inhibit auxin feedback on PIN-dependent auxin transport canalization. Nature Communications **11**, 3508.

Zhang Y, Lv S, Wang G. 2018. Strigolactones are common regulators in induction of stomatal closure *in planta*. Plant Signaling & Behavior **13**, e1444322.

FIGURE LEGENDS

Figure 1. Treatment with exogenous strigolactones induces the accumulation of ABCG25 at the plasma membrane. Left panel: Six-day-old seedlings of wild type *A. thaliana* expressing the GFP:ABCG25 construct (GFP:ABCG25/wt) were incubated in 0.5X MS media containing 0.1% acetone (MT), ABA (10 µM), or GR24^{5DS} (5DS, 10 µM) for 4 h, and the localisation of the fluorescent protein observed at the confocal microscope. **Right panel:** Histogram showing the quantification of the relative GFP signal intensity between the cytosol (cyt) and plasma membrane (PM) in GFP:ABCG25/wt seedlings treated as in the left-hand images. Data represent the mean ± SE of n = 35 cells belonging to 4 biological replicates (individual seedlings); different letters show statistical differences among treatments using Student's t-test, P-value < 0.05. Bars = 10 µm.

Figure 2. The synthesis and perception of strigolactones promote ABCG25 localisation at the plasma membrane. (A) Left panel: Six-day-old wild type (wt), *max3-11* (strigolactone-depleted, *max3*) or *d14-1* (strigolactone-insensitive, *d14*) lines expressing the GFP:ABCG25 construct were incubated in 0.5X MS media for 4 h, and the localisation of the fluorescent protein was observed at the confocal microscope. **Right panel:** Histogram showing the quantification of the relative cytosol/plasma membrane (cyt/PM) ratios of GFP signal intensity in root cells of seedlings in the left-hand images. **(B) Left panel:** Six-day-old GFP:ABCG25/*max3* seedlings were incubated in 0.5X MS media containing 0.1% acetone (mock-treated, MT), ABA (10 µM), or GR24^{5DS} (5DS, 10 µM) for 4 h, and the localization of the fluorescent protein was observed at the confocal microscope. **Right panel:** Histogram showing the quantification of the relative cyt/PM ratios of GFP signal intensity in GFP:ABCG25/*max3* seedlings treated as in the left-hand images; both strigolactones and ABA are still able to promote the localisation of ABCG25 at the plasma membrane in the *max3-11* line. **(C) Left panel:** Six-day-old GFP:ABCG25/*d14* seedlings were treated and observed as in (B). **Right panel:** Histogram showing the quantification of the relative cyt/PM ratios of GFP signal intensity in GFP:ABCG25/*d14* seedlings treated as in the left-hand images; ABA, but not strigolactones, promote the localisation of ABCG25 at the plasma membrane in the *d14-1* line. Data represent the mean ± SE of n = 35 cells belonging to 4 biological replicates (individual seedlings); different letters show overall statistical differences among treatments using Student's t-test, P-value < 0.05. Bars = 10 µm.

Figure 3: Treatment with exogenous strigolactones does not affect endocytosis but enhances ABCG25 recycling from endosomes. **(A) Left panel:** Six-day-old GFP:ABCG25/wt seedlings were first incubated in 0.5X MS media containing 0.1% acetone (mock-treated, MT), ABA (10 µM), or GR24^{5DS} (5DS, 10 µM) for 4 h and then immersed in a solution containing 50 µM Brefeldin A (BFA) for 30 min; b = BFA body. **Right panel:** Histogram showing the ratio of GFP signal intensity between cytosol and plasma membrane (cyt/PM) in GFP:ABCG25/wt seedlings treated as in the left-hand images. **(B) Left panel:** GFP:ABCG25/wt seedlings that had been immersed in a solution containing 50 µM BFA for 1 h were then incubated in the same BFA

solution (BFA→BFA) or 0.5X MS media as in (A) (BFA→MT, BFA→5DS, BFA→ABA) for 1 or 2 h. **Right panel:** Graph showing the cyt/PM ratio of GFP signal intensity in GFP:ABCG25/wt seedlings treated as in the left-hand images. The localisation of GFP:ABCG25 fluorescence was observed immediately before (0 h), 1 or 2 h after the beginning of the BFA washout. Different colours and letters show statistical differences among treatments within the same time point as determined by Student's t-test; P-value<0.05. Data represent the mean of n = 35 or n = 24 cells [in (A) and (B), respectively] belonging to 4 biological replicates (individual seedlings) for each treatment and time point. Bars = 10 µm.

Figure 4: The perception of strigolactones is necessary for GR24^{5DS} to promote ABCG25 recycling to the plasma membrane. Left panel: GFP:ABCG25/*d14* seedlings that had been immersed in a solution containing 50 µM BFA for 1 h were then incubated in the same BFA solution (BFA→BFA) or 0.5X MS media as in Fig. 3A (BFA→MT, BFA→5DS, BFA→ABA) for 1 or 2 h. Bars = 10 µm. **Right panel:** Graph showing the cyt/PM ratio of GFP signal intensity in GFP:ABCG25/*d14* seedlings treated as in the left-hand images. The localisation of GFP:ABCG25 fluorescence was observed immediately before (0 h), 1 or 2 h after the beginning of the BFA washout. Different colours and letters show statistical differences among treatments within the same time point as determined by Student's t-test; P-value<0.05. Data represent the mean of n = 24 cells belonging to 4 biological replicates (individual seedlings) for each treatment and time point.

Figure 5: Osmotic stress downregulates the strigolactone biosynthetic genes *MAX3* and *MAX4* in *A. thaliana* roots. Relative transcript amounts of *MAX3*, *MAX4*, *NCED3*, *RD29B* and *ABCG25* in 6-day-old rootlets subjected to PEG treatment for 30 min, 1 or 3 h were normalised on the corresponding mock-treated control in water. Relative expression levels were calculated using the geometric means of *AtTUA4* and *AtUBQ10* transcript concentrations as reference (**Supplementary Table S1**). Data represent the mean ± SE of at least 3 biological replicates for each condition (each replicate the pool of over 50 rootlets) and time point. Different letters indicate statistically significant differences across time points assessed by Student's t-test; P value < 0.05.

Figure 6: The endocytosis of ABCG25 in *A. thaliana* seedlings under osmotic stress is faster in strigolactone-insensitive roots. **Left panel:** *A. thaliana* seedlings expressing the GFP:ABCG25 construct in the **(A)** wild type or **(B)** strigolactone-insensitive genotype *d14-1* were incubated in water (mock-treated, MT) or in a 20% PEG solution, and roots were observed at the confocal microscope after 1, 2 and 3 h. **Right panel:** The cytosol/plasma membrane (cyt/PM) GFP fluorescence ratio was calculated in root cells of GFP:ABCG25/wt **(A)** or GFP:ABCG25/*d14* **(B)** subjected to mock or PEG treatment. In (A) and (B) the "before treatment" label indicates ratio values right before the beginning of either treatment. **(C)** Normalisation of the cyt/PM GFP signal ratio of each time point of PEG treatment on the respective control in the wild type (black bars) or *d14-1* background (white bars). The "before treatment" values of each genotype are normalised on their own averages and thus, are set to 1. Bars in graphs represent the mean ± SE of n = 35

cells belonging to 4 biological replicates (individual seedlings). Different letters show statistical differences among treatments and time points using Kruskal-Wallis and post-hoc test, P value < 0.05; n = nucleus, v = vacuole; bars = 10 µm.

Figure 7: Exogenous strigolactones modulate ABA levels in roots, partly in dependence of ABCG25. Four-week-old wild type and *abcg25-5* mutant plantlets grown in agar plates were sprayed with 10 µM $GR24^{5DS}$ solution (5DS), while controls were sprayed with a mock solution (0.1% of acetone in water); 24 h later, osmotic stress was induced by spraying a 20% PEG solution while controls were sprayed with water. ABA was quantified by LC-MS on tissues sampled 24 h later. Treatment with $GR24^{5DS}$ tended to increase total ABA in wild-type root tissues (black bars), especially if followed by PEG treatment. This was not seen in the absence of the ABCG25 protein (striped bars), when $GR24^{5DS}$ decreased total ABA content. Different letters on top of bars indicate statistical differences among treatments, according to Three-Way ANOVA analysis (P value < 0.05).

Figure 8: The internalisation of ABCG25 in *A. thaliana* roots under osmotic stress is favoured by the repression of strigolactone synthesis. Under regular conditions of water availability (**left**), the steady-state levels of strigolactones (SL) in root cells ensures that a proper amount of the ABA exporter protein ABCG25 is localised at the plasma membrane via efficient endosomal recycling; thus, endocellular ABA levels are kept low. This is consistent with the effects of treatment with the strigolactone analogue $GR24^{5DS}$ and with the phenotype of plants defective in strigolactone synthesis or perception. When osmotic stress occurs (**right**), strigolactone synthesis is quickly repressed in roots of Arabidopsis and other plants, favouring the internalisation of ABCG25 and the increase in endocellular ABA needed for local acclimation responses. Strigolactone-insensitive plants such as *d14-1* display, as expected, less ABCG25 at the plasma membrane of root cells under normal conditions, and faster ABCG25 internalisation in root cells during early osmotic stress than the wild type. Other regulation levels (i.e., on the transcription of ABA biosynthetic genes, or on sensitivity to ABA) are of course possible but not included in the model.

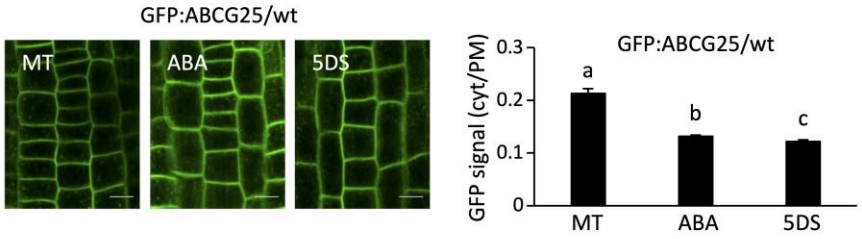

Figure 1. Treatment with exogenous strigolactones induces the accumulation of ABCG25 at the plasma membrane. Left panel: Six-day-old seedlings of wild type *A. thaliana* expressing the GFP:ABCG25 construct (GFP:ABCG25/wt) were incubated in 0.5X MS media containing 0.1% acetone (MT), ABA (10 µM), or $GR24^{5DS}$ (5DS, 10 µM) for 4 h, and the localisation of the fluorescent protein observed at the confocal microscope. **Right panel:** Histogram showing the quantification of the relative GFP signal intensity between the cytosol (cyt) and plasma membrane (PM) in GFP:ABCG25/wt seedlings treated as in the left-hand images. Data represent the mean ± SE of n = 35 cells belonging to 4 biological replicates (individual seedlings); different letters show statistical differences among treatments using Student's t-test, P-value < 0.05. Bars = 10 µm.

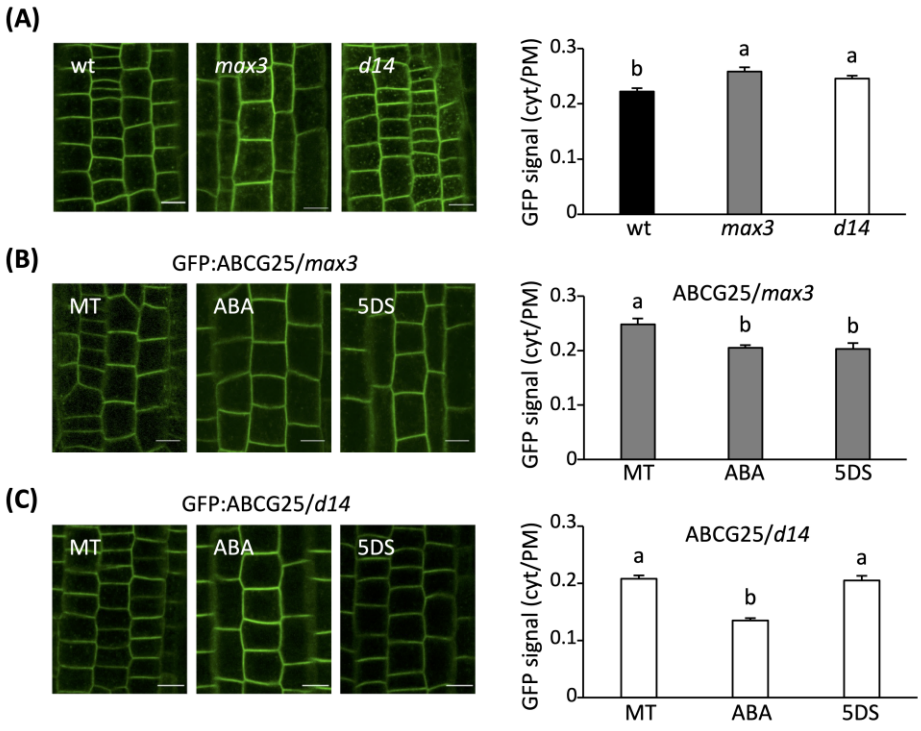

Figure 2. The synthesis and perception of strigolactones promote ABCG25 localisation at the plasma membrane. (A) Left panel: Six-day-old wild type (wt), *max3-11* (strigolactone-depleted, *max3*) or *d14-1* (strigolactone-insensitive, *d14*) lines expressing the GFP:ABCG25 construct were incubated in 0.5X MS media for 4 h, and the localisation of the fluorescent protein was observed at the confocal microscope. **Right panel:** Histogram showing the quantification of the relative cytosol/plasma membrane (cyt/PM) ratios of GFP signal intensity in root cells of seedlings in the left-hand images. **(B) Left panel:** Six-day-old GFP:ABCG25/*max3* seedlings were incubated in 0.5X MS media containing 0.1% acetone (mock-treated, MT), ABA (10 µM), or $GR24^{5DS}$ (5DS, 10 µM) for 4 h, and the localization of the fluorescent protein was observed at the confocal microscope. **Right panel:** Histogram showing the quantification of the relative cyt/PM ratios of GFP signal intensity in GFP:ABCG25/*max3* seedlings treated as in the left-hand images; both strigolactones and ABA are still able to promote the localisation of ABCG25 at the plasma membrane in the *max3-11* line. **(C) Left panel:** Six-day-old GFP:ABCG25/*d14* seedlings were treated and observed as in (B). **Right panel:** Histogram showing the quantification of the relative cyt/PM ratios of GFP signal intensity in GFP:ABCG25/*d14* seedlings treated as in the left-hand images; ABA, but not strigolactones, promote the localisation of ABCG25 at the plasma membrane in the *d14-1* line. Data represent the mean ± SE of n = 35 cells belonging to 4 biological replicates (individual seedlings); different letters show overall statistical differences among treatments using Student's t-test, P-value < 0.05. Bars = 10 µm.

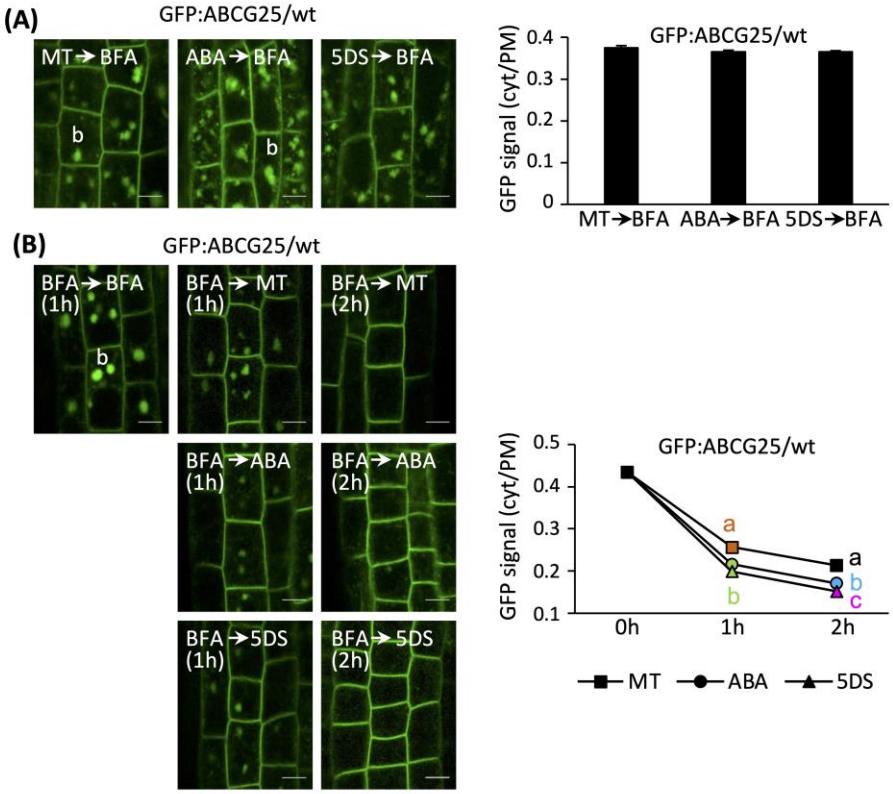

Figure 3: Treatment with exogenous strigolactones does not affect endocytosis but enhances ABCG25 recycling from endosomes. **(A) Left panel:** Six-day-old GFP:ABCG25/wt seedlings were first incubated in 0.5X MS media containing 0.1% acetone (mock-treated, MT), ABA (10 µM), or $GR24^{5DS}$ (5DS, 10 µM) for 4 h and then immersed in a solution containing 50 µM Brefeldin A (BFA) for 30 min; b = BFA body. **Right panel:** Histogram showing the ratio of GFP signal intensity between cytosol and plasma membrane (cyt/PM) in GFP:ABCG25/wt seedlings treated as in the left-hand images. **(B) Left panel:** GFP:ABCG25/wt seedlings that had been immersed in a solution containing 50 µM BFA for 1 h were then incubated in the same BFA solution (BFA→BFA) or 0.5X MS media as in (A) (BFA→MT, BFA→5DS, BFA→ABA) for 1 or 2 h. **Right panel:** Graph showing the cyt/PM ratio of GFP signal intensity in GFP:ABCG25/wt seedlings treated as in the left-hand images. The localisation of GFP:ABCG25 fluorescence was observed immediately before (0 h), 1 or 2 h after the beginning of the BFA washout. Different colours and letters show statistical differences among treatments within the same time point as determined by Student's t-test; P-value<0.05. Data represent the mean of n = 35 or n = 24 cells [in (A) and (B), respectively] belonging to 4 biological replicates (individual seedlings) for each treatment and time point. Bars = 10 µm.

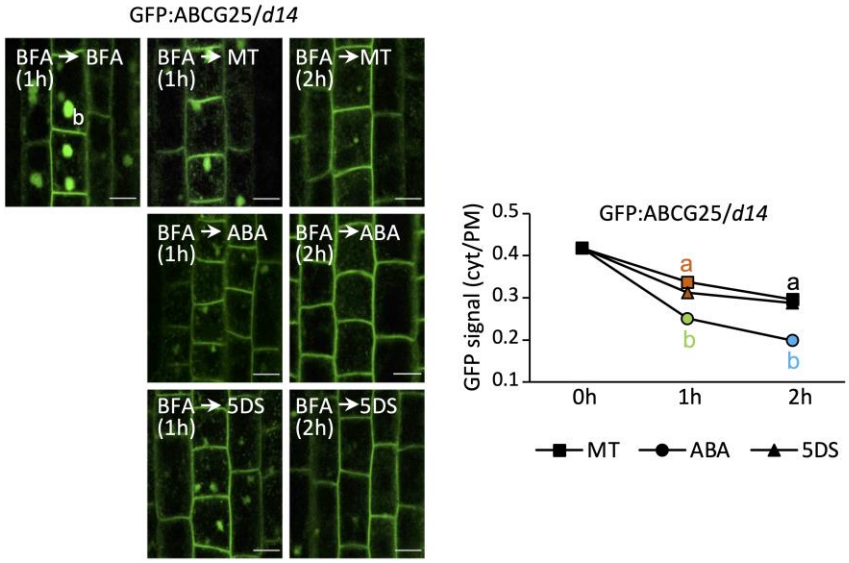

Figure 4: The perception of strigolactones is necessary for GR24^{5DS} to promote ABCG25 recycling to the plasma membrane. Left panel: GFP:ABCG25/*d14* seedlings that had been immersed in a solution containing 50 µM BFA for 1 h were then incubated in the same BFA solution (BFA→BFA) or 0.5X MS media as in Fig. 3A (BFA→MT, BFA→5DS, BFA→ABA) for 1 or 2 h. Bars = 10 µm. **Right panel:** Graph showing the cyt/PM ratio of GFP signal intensity in GFP:ABCG25/*d14* seedlings treated as in the left-hand images. The localisation of GFP:ABCG25 fluorescence was observed immediately before (0 h), 1 or 2 h after the beginning of the BFA washout. Different colours and letters show statistical differences among treatments within the same time point as determined by Student's t-test; P-value<0.05. Data represent the mean of n = 24 cells belonging to 4 biological replicates (individual seedlings) for each treatment and time point.

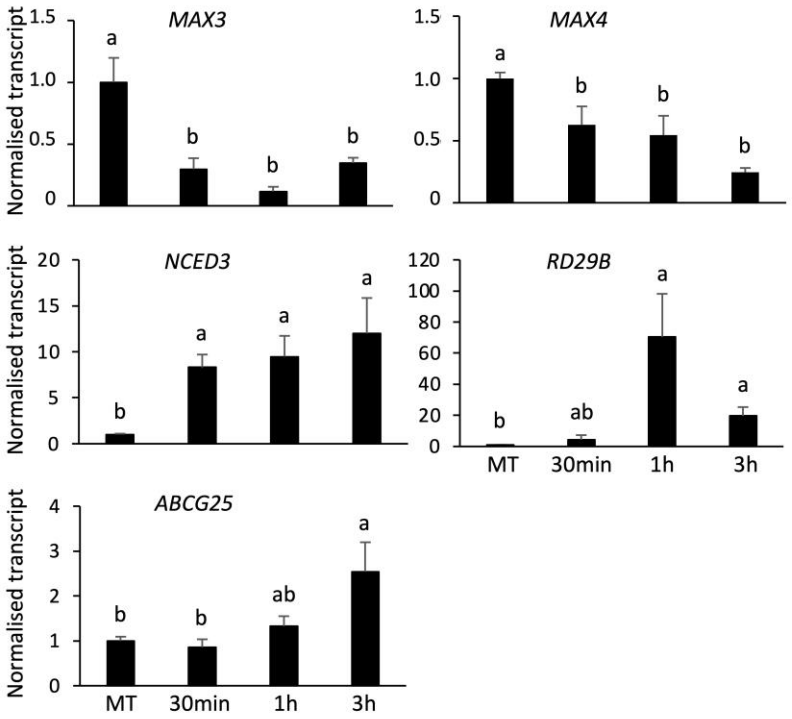

Figure 5: Osmotic stress downregulates the strigolactone biosynthetic genes *MAX3* and *MAX4* in *A. thaliana* roots. Relative transcript amounts of *MAX3*, *MAX4*, *NCED3*, *RD29B* and *ABCG25* in 6-day-old rootlets subjected to PEG treatment for 30 min, 1 or 3 h were normalised on the corresponding mock-treated control in water. Relative expression levels were calculated using the geometric means of *AtTUA4* and *AtUBQ10* transcript concentrations as reference (**Supplementary Table S1**). Data represent the mean ± SE of at least 3 biological replicates for each condition (each replicate the pool of over 50 rootlets) and time point. Different letters indicate statistically significant differences across time points assessed by Student's t-tests; P value < 0.05.

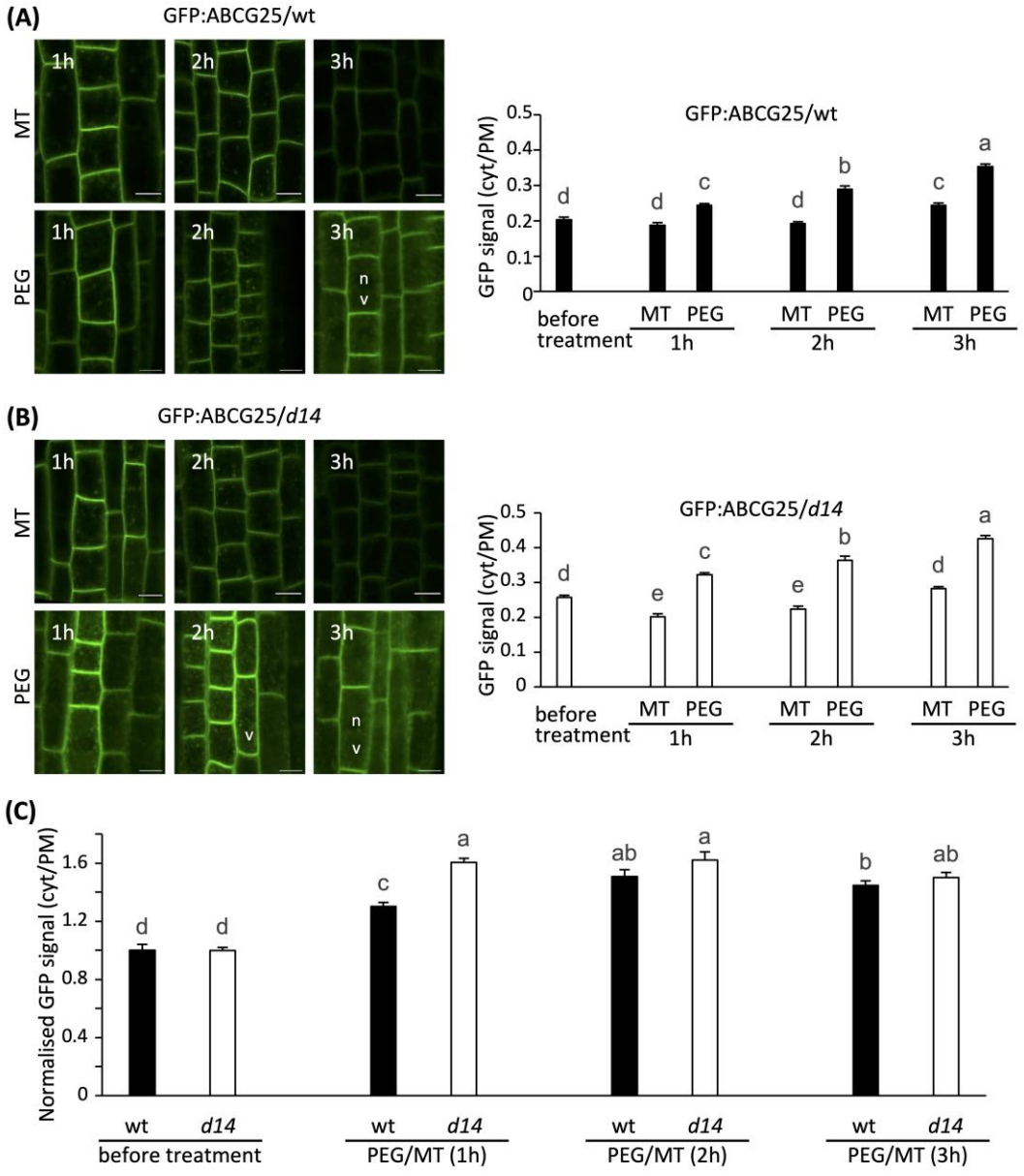

Figure 6: The endocytosis of ABCG25 in *A. thaliana* seedlings under osmotic stress is faster in strigolactone-insensitive roots. **Left panel:** *A. thaliana* seedlings expressing the GFP:ABCG25 construct in the **(A)** wild type or **(B)** strigolactone-insensitive genotype *d14-1* were incubated in water (mock-treated, MT) or in a 20% PEG solution, and roots were observed at the confocal microscope after 1, 2 and 3 h. **Right panel:** The cytosol/plasma membrane (cyt/PM) GFP fluorescence ratio was calculated in root cells of GFP:ABCG25/wt **(A)** or GFP:ABCG25/*d14* **(B)** subjected to mock or PEG treatment. In (A) and (B) the "before treatment" label indicates ratio values right before the beginning of either treatment. **(C)** Normalisation of the cyt/PM GFP signal ratio of each time point of PEG treatment on the respective control in the wild type (black bars) or *d14-1* background (white bars). The "before treatment" values of each genotype are normalised on their own averages and thus, are set to 1. Bars in graphs represent the mean ± SE of n = 35 cells belonging to 4 biological replicates (individual seedlings). Different letters show statistical differences among treatments and time points using Kruskal-Wallis and post-hoc test, P value < 0.05; n = nucleus, v = vacuole; bars = 10 µm.

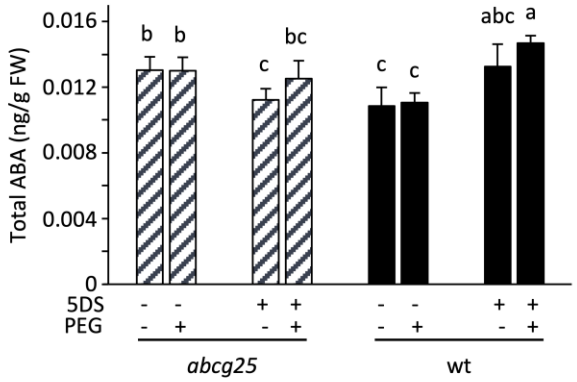

Figure 7: Exogenous strigolactones modulate ABA levels in roots, partly in dependence of ABCG25. Four-week-old wild type and *abcg25-5* mutant plantlets grown in agar plates were sprayed with 10 µM $GR24^{5DS}$ solution (5DS), while controls were sprayed with a mock solution (0.1% of acetone in water); 24 h later, osmotic stress was induced by spraying a 20% PEG solution while controls were sprayed with water. ABA was quantified by LC-MS on tissues sampled 24 h later. Treatment with $GR24^{5DS}$ tended to increase total ABA in wild-type root tissues (black bars), especially if followed by PEG treatment. This was not seen in the absence of the ABCG25 protein (striped bars), when $GR24^{5DS}$ decreased total ABA content. Different letters on top of bars indicate statistical differences among treatments, according to Three-Way ANOVA analysis (P value < 0.05).

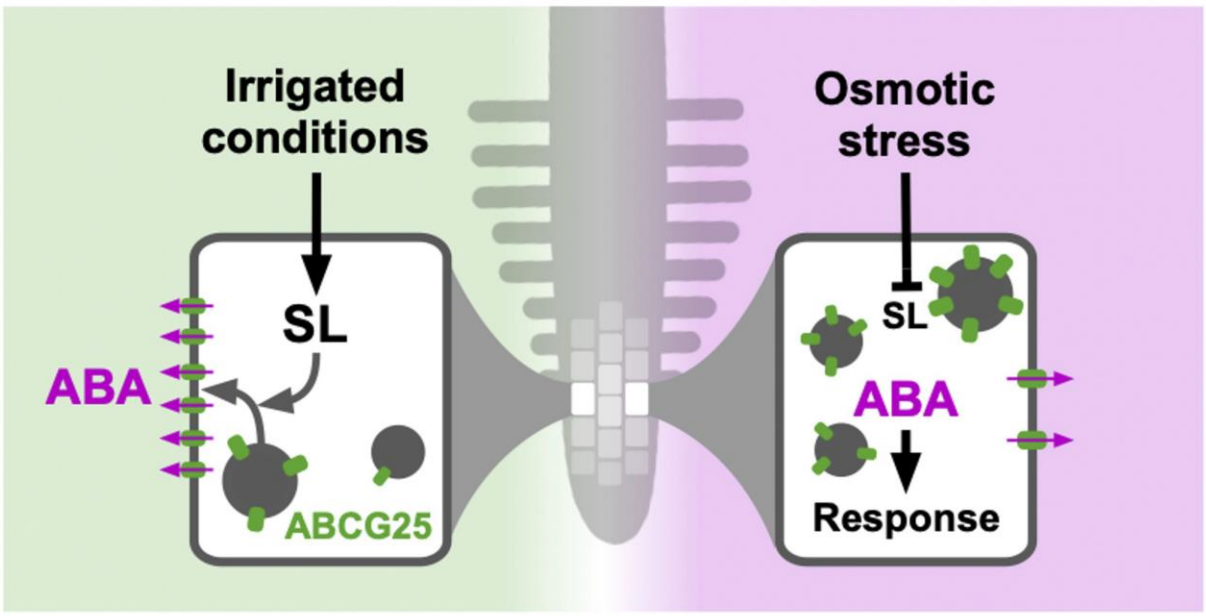

Figure 8: The internalisation of ABCG25 in *A. thaliana* roots under osmotic stress is favoured by the repression of strigolactone synthesis. Under regular conditions of water availability (**left**), the steady-state levels of strigolactones (SL) in root cells ensures that a proper amount of the ABA exporter protein ABCG25 is localised at the plasma membrane via efficient endosomal recycling; thus, endocellular ABA levels are kept low. This is consistent with the effects of treatment with the strigolactone analogue $GR24^{5DS}$ and with the phenotype of plants defective in strigolactone synthesis or perception. When osmotic stress occurs (**right**), strigolactone synthesis is quickly repressed in roots of Arabidopsis and other plants, favouring the internalisation of ABCG25 and the increase in endocellular ABA needed for local acclimation responses. Strigolactone-insensitive plants such as *d14-1* display, as expected, less ABCG25 at the plasma membrane of root cells under normal conditions, and faster ABCG25 internalisation in root cells during early osmotic stress than the wild type. Other regulation levels (i.e., on the transcription of ABA biosynthetic genes, or on sensitivity to ABA) are of course possible but not included in the model.